Characterizing major avalanche episodes in space and time in the twentieth and early twenty-first centuries in the Catalan Pyrenees

Pere Oller[1], Elena Muntán[2], Carles García-Sellés[1], Glòria Furdada[2], Cristina Baeza[3], Cecilio Angulo[3]
[1] Institut Geològic de Catalunya, Barcelona, Catalonia, Spain.
[2] Universitat de Barcelona, Barcelona, Catalonia, Spain.
[3] Universitat Politècnica de Catalunya, Barcelona, Catalonia, Spain.

ABSTRACT: With the aim of better understanding avalanche risk in the Catalan Pyrenees, the present work focuses on the analysis of major (or destructive) avalanches. For such purpose major avalanche cartography was made by an exhaustive photointerpretation of several flights, winter and summer field surveys and inquiries to local population. Major avalanche events were used to quantify the magnitude of the episodes during which they occurred and an Avalanche Magnitude Index (AMI) was developed. This index is based on the number of major avalanches registered and its estimated frequency in a given time period, and it quantifies the magnitude of a major avalanche episode or winter. Furthermore, it allows comparing the magnitude between major avalanche episodes in a given mountain range, or between mountain ranges. Major episodes from winter 1995/96 to the present were reconstructed. Their magnitude, frequency and extent were also assessed. During the last 18 winters, the episodes of January 22-23 and February 6-8 in 1996 were those with highest AMI values, followed by January 30-31, 2003, and January 29, 2006. With less accuracy, the same parameters were obtained at winter time resolution throughout the twentieth century. Again, 1996 winter had the highest AMI value followed by 1971/72, 1974/75 and 1937/38 winter seasons. The analysis of the spatial extent of the different episodes allowed refining the demarcation of nivological regions, and improving our knowledge about the atmospheric patterns that cause major episodes.

KEYWORDS: Major avalanche, Pyrenees, magnitude, frequency, hazard, risk.

1 INTRODUCTION

We analyzed individual major avalanches to quantify the magnitude and frequency of major avalanche episodes in the Catalan Pyrenees. We considered "major avalanche" (MA) as the avalanche which extent exceeds the reach of the usual (frequent) avalanches, causing damage in case there is forest or infrastructures in the vicinity (Schaerer, 1986). We observed that these avalanches typically have a return period over 10 years. We considered a "major avalanche episode" (MAE) as the period in which the release of one or more MA occurs due to snowpack instability caused by one nivometeorological scenario. It can last from a few hours to several days.

We worked with MA because they cause damage and therefore risk, and because this fact makes it easier to collect a complete data set of avalanches obtained from a threshold defined by the existence of damage, considering it as an exceedance probability (McClung, 2008).

Corresponding author address: Pere Oller, Institut Geològic de Catalunya, Barcelona, Catalonia, Spain;
tel: +34 935538430;
email: pereo@igc.cat

The objectives of this paper were: (i) to reconstruct the MAE occurred over the Pyrenees of Catalonia during the twentieth and early twenty-first century, (ii) to determine its magnitude, (iii) its frequency and (iv) its spatial extent.

2 STUDY AREA

The study area comprises the Catalan Pyrenees, or southeastern part of the Pyrenean range (Figure 1), an area of 5000 km^2. The highest peaks just exceed 3000 m a.s.l., and the timber line oscillates between 2100 and 2500 m (Carreras et al, 1996). Where the terrain is prone to avalanche release, in absence of forest cover, avalanches can trigger from above 1400 m a.s.l., and they can reach elevations as low as 600 m a.s.l. (Oller et al., 2006).

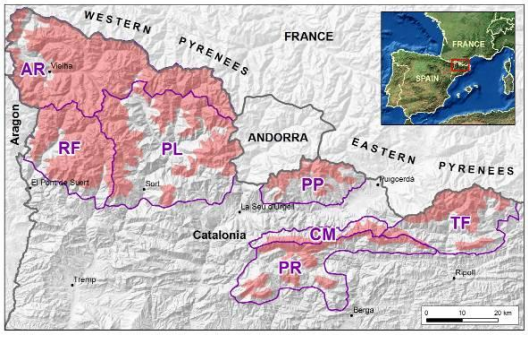

Figure 1. Location of the Catalan Pyrenees and areas susceptible to avalanche activity (shaded

in red). Nivological regions are demarcated by violet boundaries: AR (Aran-Franja nord de la Pallaresa), RF (Ribagorçana-Vall Fosca), PL (Pallaresa), PP (Perafita-Puigpedrós), CM (Vessant nord del Cadí-Moixeró), PR (Prepirineu), TF (Ter-Freser).

2.1 Snow and climate regions

In 1994 the Catalan Pyrenees were divided into 7 nivological regions (NR, Figure 1) based on climate characteristics, snowpack evolution and avalanche activity (García et al., 2007). Three climate varieties were defined. The northwestern part has a humid oceanic climate with regular winter precipitation (AR region). Towards the south of the western Catalan Pyrenees, the weather gains continental traits, and winter precipitation decreases (RF, PL, PP and CM regions). In eastern Pyrenees the Mediterranean influence takes predominance. Winter precipitation increases though irregularly distributed (PR and TF regions).

Garcia et al (2009) identified the atmospheric patterns which generate MAE over the Pyrenees of Catalonia. They worked with 25 episodes from 1972 to 2007 (35 winters). They obtained 6 atmospheric patterns that cause major avalanche episodes at synoptic scale at a geopotential height of 500 hPa (table 1). This classification was used in the present work to analyse the selected MAE.

Comp.	Low levels synoptic config.	Nr.	Snow and avalanche conditions	Typical NR	Acronym
1	N and NW advection	12	Intense snowfalls, very low temp, very active snowdrift. Major powder avalanches, sometimes wet.	AR	E_N/NW
2	SE advection	4	Weak layers in the snowpack. Heavy precipitation. Dense flow avalanches	PR, TF	E_E/SE1
3	E and SE advection	4	Intense snowfalls, mild temperatures. Dense dry and wet avalanches	PR, TF, RF	E_E/SE2
4	N and NE advection	1	Northern Strong winds and heavy snowfalls. Major powder avalanches	Any region	E_NE
5	S and SW advection	2	Very intense precipitation, mild temperatures. Dense dry and wet avalanches	PR, CM, RF, TF	E_S/SW
6	Worm advection	2	Sudden melting processes on snow cover which contains persistent weak layers	Any region	E_AC

Table 1. Atmospheric patterns found by García et al., (2009).

3 MATERIALS AND METHODS

3.1 Major avalanche data

We worked with avalanches recorded in the Avalanche Database of Catalonia (BDAC) of the Geological Institute of Catalonia (IGC; Oller et al., 2005). Data was collected over the past 25 years. Additional work was made to prepare data for treatment in the present study: (i) selection of major avalanches, (ii) debugging data to avoid mistakes and repetitions and (iii) completing the series from field work, inquiries to population and photointerpretation. We collected an inventory consisting of 514 major avalanches, 349 of which dated at winter season resolution.

Based on the completeness of the series, we defined 3 periods: (i) P1, with very sporadic records prior to the twentieth century obtained from historical documents largely. Usually they are isolated events that affect localities. The oldest events are dated to the fifteenth century; (ii) P2, which covers the twentieth century, until winter 1994/95. For the most part, the record was obtained from inquiries to the local population, but also from dendrochronological analyses (Muntán et al., 2004 and 2009). The dataset is incomplete but probably the most important events were registered. P3 (iii), from winter 1995/96 to the present, the registration of MA can be considered systematic and complete.

Avalanches were mapped from the observation of phenomena and evidence on the vegetation and infrastructures. We worked with P2 and P3 data as it was considered that the series were reasonably complete with respect to the episodes of greater magnitude as discussed in this work (Figure 2).

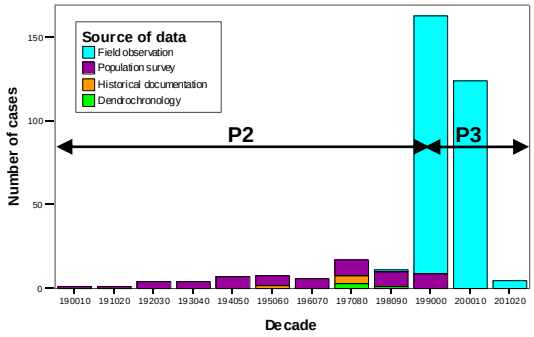

Figure 2. Decadal distribution of MA recorded and source of the data in P2 and P3 periods.

3.2 Data treatment

We worked with the periods P3 and P2+P3, separately, taking into account the different resolution of the data. The common parameters for both periods, useful for the goal of this work were the spatial distribution, the temporal distribution and the runout distance.

3.2.1 Spatial and temporal distribution

All the registered events were georeferenced according to their X and Y coordinates.

The winter season was considered the time unit for working in P2+P3. This fact forced us to discard many events in P2 that were not possible to date at that resolution. However, in P3,

most of the events were dated at MAE time resolution.

3.2.2 *Runout distance*

This is the most sensitive parameter, because accuracy is variable depending on the source of information. The runout distance considered was determined from the destructive effects of the avalanche. This is the only common parameter for both periods, P2 and P3. Actually, what we compared is the minimum extent of the avalanche (Corona et al., 2012). The observed effects often do not correspond to the real extent of the avalanche, but to the part of the avalanche with destructive power. In case of a powder avalanche, the extent of the mapped avalanche will be located in an intermediate point between the extent of the dense part and that of the powder part. In the case of the historical method, witnesses may refer to the destruction of a house, which could not coincide with the full extent of the avalanche, or may refer to the extent of the powder part, which in its most distal part causes no damage. It should be noted that the range of uncertainty is significant, and it must be taken into account in the interpretation of results.

The extent of the different events for each avalanche path was mapped on the digital topographic and orthophoto bases 1:5000 of the Cartographic Institute of Catalonia (ICC), as shown in the example of figure 3.

3.2.3 *Frequency/Intensity*

The relationship frequency/intensity of each event was obtained from the relative position of the different distances measured in the runout zone (Figure 3). In general it is expected that in a given avalanche path, as the average intensity increases downhill in the runout zone, the average frequency decreases (McClung, 2008). Thus, the intensity is determined indirectly from the observed frequency. The parameter used to find out this relationship was the relative runout distance between different events, in relation to the frequency of occurrence in each avalanche path.

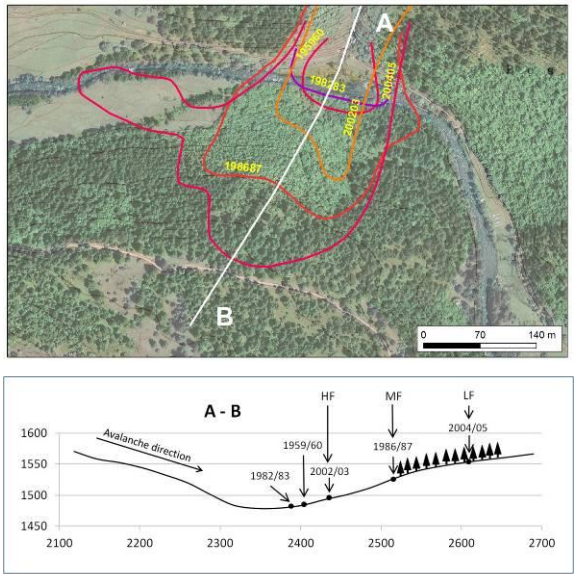

Figure 3. Example of runout distances reached by different avalanches in a given avalanche path, mapped (up) and plotted in a topgraphic profile (down). HF, MF and LF: high, medium and low frequency.

The return period is the time interval in which the runout distance is achieved or exceeded in a given point. Frequency is the reciprocal of the return period. It is therefore possible, in principle, to map return periods in the runout zone corresponding to different distances downhill, for example, 1 year, 10 years, 100 years, corresponding to a mean annual probability of 1, 0.1 , 0.01. These distances increase in the runout zone at the same time that the return period increases (McClung and Schaerer, 2006). Given the lack of data generally everywhere, avalanche frequency can be estimated as an order of magnitude (Weir, 2002; Mears, 1992).

Based on the classification table of mountain hazards by Weir (2002), a classification of the avalanche frequency was defined for each avalanche path (Table 2).

Frequency classes	Return period (y)	Annual probability of occurrence
Very high (VHF)	5 (1-10)	0,2 (1-0,1)
High (HF)	10 (5-30)	0,1 (0,2-0,03)
Moderate (MF)	30 (10-100)	0,03 (0,1-0,01)
Low (LF)	100 (30-300)	0,01 (0,03-0,003)
Very low (VLF)	300 (>100)	<0,003 (<0,01)

Table 2. Frequency classes established for the treated avalanches (based on Weir, 2002). Values in parentheses indicate the range of uncertainty.

To determine the frequency in the runout zone 3 criteria (absolute and relative) were considered: (i) number of times that events with similar runout distances were repeated in relation to the lapse of time between them (absolute), (ii) vegetation clues as a reference (abso-

lute), and (iii) space/time relationship between runout distances of avalanches recorded in each avalanche path (relative).

Very high frequency avalanches were not considered MA according to the criteria used in this study. There are no cases in which these avalanches have affected forest. However, in forested areas, high frequency avalanches affect forest often, but this is not the rule. At least 20% of the high frequency avalanches recorded, did not affect forest. This means that possibly the record of high frequency avalanches is not complete in P3 (we cannot guarantee a complete record if there are no evidences). On the contrary, we consider that the register of moderate to very low frequency avalanches is almost complete in P3 (figure 4).

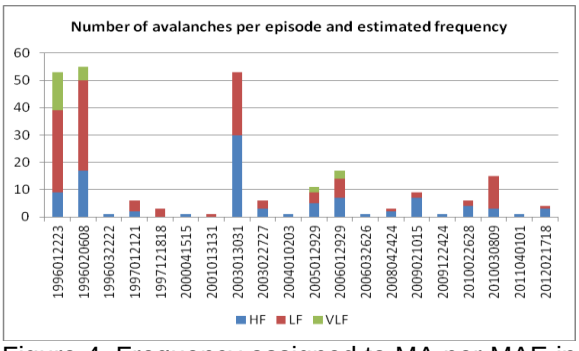

Figure 4. Frequency assigned to MA per MAE in P3 period. Date of episodes has the format YYYYMMD$_1$D$_1$D$_2$D$_2$, where D$_1$D$_1$ is the first and D$_2$D$_2$ the last day of the episode.

4 ANALYSIS AND RESULTS

4.1 Analysis of the period P3

A primary objective of this study was to quantify the magnitude of the registered MAE. For such a purpose an index was conceived, similarly to Schweizer et al. (1998) and Haegeli and McClung (2003). In the case of these authors, they applied an index on a daily basis (Avalanche Activity Index, AAI), that is to get a value of the daily activity of avalanches. They based it on the avalanche size, according to the Canadian avalanche size scale (McClung and Schaerer, 2006). They used the sum of all observed avalanches considering a weight according to its size. These weights were 0.01, 0.1, 1 and 10 for sizes 1 to 4 respectively, assuming that the mass and therefore the power of an avalanche is increased by 10 from one size to the next. In our case, since we only worked with MA, mostly sizes 3 and 4, we used the frequency to emphasize the exceptionality of the episode. Major avalanches were classified in 4 classes (from 2, high frequency, to 5, very low frequency) and a weight inversely proportional to the estimated frequency of each avalanche was assigned (0.1, 0.3, 1 and 3). Like that we gave prominence to the lower frequency avalanches, the most intense. The obtained parameter was called Avalanche Magnitude Index (AMI).

The AMI can be applied to the time scale allowed by the data resolution, e. g., episode, month, winter. In P3 we could apply this index at MAE resolution following the expression 1.

$$AMIe = \left[\left(\frac{N_{HF}e}{\max\left(N_{HF}e\right)} \cdot 0{,}1\right) + \left(\frac{N_{MF}e}{\max\left(N_{MF}e\right)} \cdot 0{,}3\right) + \left(\frac{N_{LF}e}{\max\left(N_{LF}e\right)} \cdot 1\right) + \left(\frac{N_{VLF}e}{\max\left(N_{VLF}e\right)} \cdot 3\right)\right] / 4{,}4 \quad (1)$$

For each episode (*e*), avalanches were grouped according to their frequency and were divided by its maximum value registered in the dataset for standardization. $N_{HF}e$ is the number of high frequency MA recorded in an episode *e*, and max($N_{HF}e$) is the maximum number of recorded high frequency MA in a MAE. The resulting value for each frequency class is multiplied by the weight assigned to it. The final value is divided by 4.4, to obtain a result between 0 and 1.

The AMI*e* also becomes an index of the exceptionality of the MAE of the analyzed period. The obtained values respond to a logarithmic scale. Following the same reasoning about the weight assigned to the exceptionality of an avalanche, values were classified as shown in table 3.

AMI	
Classes	**Numerical value**
Low	<0,03
Medium	0,03 – 0,1
High	0,l – 0,3
Very high	>0,3

Table 3. AMI values classification.

In P3 period (17 winters) the AMIe was calculated for the 20 recorded episodes (Figure 5). We obtained high values for January and February 1996 episodes, even though January could be considered to be very high. The 30th and 31st January 2003, the 29th January 2005 and 29th January 2006, the AMI*e* values were medium, and for the rest of MAE values were low.

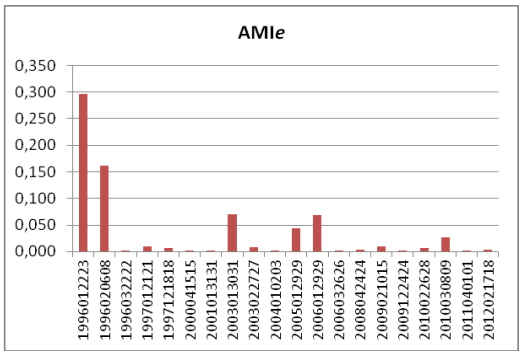

Figure 5. AMI*e* values obtained for P3.

For each episode, the extent of the area deforested by avalanches was mapped and measured (Figure 6). This parameter is also an indicator of the exceptionality of the episode. We correlated the AMI*e* values with the deforested area values and we obtained a Pearson correlation coefficient of 0.96, which reinforces the validity of the AMI*e* as an indicator of MAE magnitude.

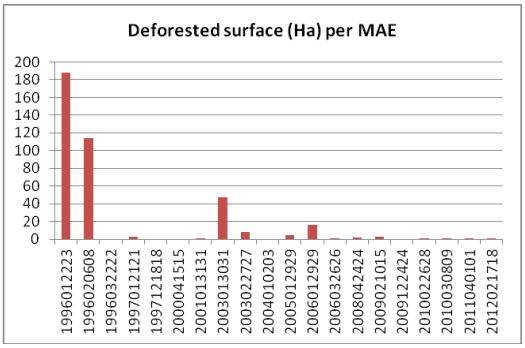

Figure 6. Deforested surface per MAE, for P3.

The obtained AMI*e* values were associated with each atmospheric circulation pattern defined by Garcia et al. (2009). In table 4 all the registered episodes, the observed dynamics per episode and the corresponding AMI*e* values are listed.

Episode	Comp.	Observed dynamics	AMI*e*
1996012223	E_S/SW	Dense dry and aerosol	0,296
1996020608	E_N/NW	Aerosol	0,162
1996032222	E_AC	Dense wet	0,001
1997012121	E_E/SE2	Dense dry and dense wet	0,010
1997121818	E_E/SE1	Slushflow	0,006
2000041515	E_S/SW	Dense wet	0,001
2001013131	E_N/NW	Aerosol	0,002
2003013031	E_N/NW	Dense dry and aerosol	0,070
2003022727	E_E/SE1	Dense dry	0,008
2004010203	E_N/NW	Aerosol	0,001
2005012929	E_N/NW	Aerosol	0,045
2006012929	E_E/SE2	Dense dry and aerosol	0,068
2006032626	E_AC	Dense wet	0,001
2008042424	E_S/SW	Dense dry	0,004
2009021015	E_N/NW	Dense dry and aerosol	0,009
2009122424	E_S/SW	Dense wet	0,001
2010022628	E_S/SW	Dense wet	0,006
2010030809	E_NE	Aerosol	0,027
2011040101	E_AC	Dense wet	0,001
2012021718	E_N/NW	Dense wet	0,003

Table 4. Registered episodes and corresponding AMI*e* values.

Figure 7 shows how MAE with greatest AMI*e* correspond to the pattern S/SW, secondly, to the pattern N/NW and E/SE2. The AMI*e* decreases considerably in NE and even more in E/SE1 MAE. It is merely testimonial in AC MAE, since in these situations major avalanches have occurred sporadically.

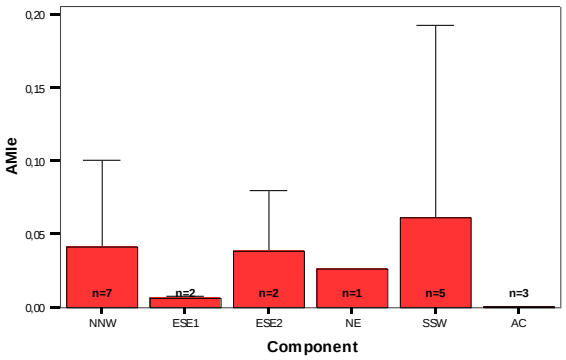

Figure 7. AMI*e* values (mean and standard deviation) related to their assigned atmospheric patterns.

In relation to the month of MAE occurrence (Figure 8), the highest values were obtained in January and February and, in decreasing order the following months until spring. In those episodes in which a powder part was observed, the AMI*e* values were the highest, indicating that these are the most intense episodes. In contrast, the more dense and wet the avalanches, the lower the AMI*e* values.

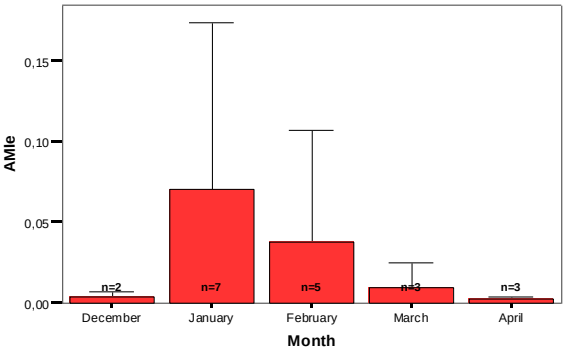

Figure 8. AMI*e* values (mean and standard deviation) related to the month of occurrence.

Considering the winter season as a temporal unit, we obtained the results shown in figure 9. From the 17 winters in P3 period, MAE were registered in 14 winters, being 1995/96 the most important, with very high AMI*w* values. On a second position, winters 2002/03, 2005/06 and 2004/05, registered medium values, and the other winters registered low AMI*w* values, despite being significative in 2009/10.

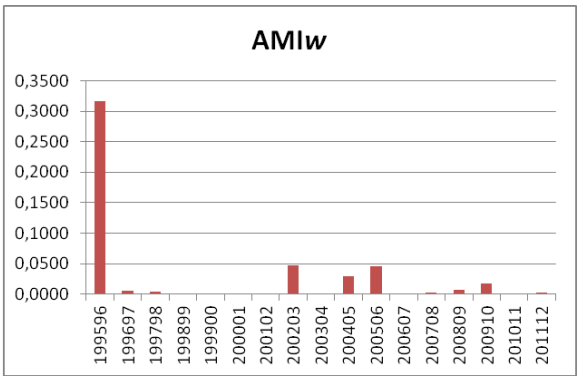

Figure 9. AMI*w* values obtained for the period P3.

4.1.2 Spatial analysis

From the spatial distribution of the MA recorded in each MAE, the affected territory was reconstructed. Our reconstruction was based on the criterion that the behavior of air masses is strongly influenced by relief, causing 50 to 70% of mountain precipitation in winter (McClung and Schaerer, 2006). This assumption is easily confirmed in the distribution of avalanches depending on the direction of the air mass that generated the MAE. Taking this into consideration, the area of each MAE was mapped (figure 10). The superimposition of all the P3 MAE (20 events) showed a higher frequency in the RF, western PL and eastern AR regions, in western Pyrenees, and TF in eastern Pyrenees. It is important to emphasize that PP region was only affected by 2 major episodes. This is the region with the lowest MAE frequency.

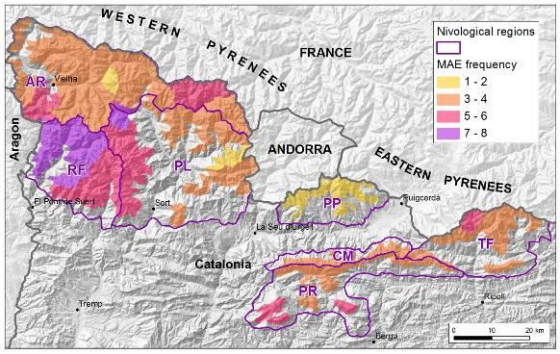

Figure 10. Map with the superimposition of all the registered MAE.

With these results the NR were redefined to better characterize the MAE spatial distribution. The new divisions were called Major Avalanche Regions (MAR). From west to east they are: GA (Garona), PN (Nord Pallaresa), RP (Ribagorçana-Pallaresa oest), PE (Pallaresa est), SN (Nord Segre), SL (Segre-Llobregat), TF (Ter-Freser) (figure 12).

These regions can also be grouped according to the climatic influence (Climatic Major Avalanche Regions, CMAR), in Oceanic influence regions, affected mainly by N/NW episodes (GA and PN); Continental influence regions, affected mainly by S/SW episodes, but also N/NW (RP, PE and SN); and Mediterranean regions, affected by a high variety of atmospheric patterns (up to 5; SL and TF, figure 11).

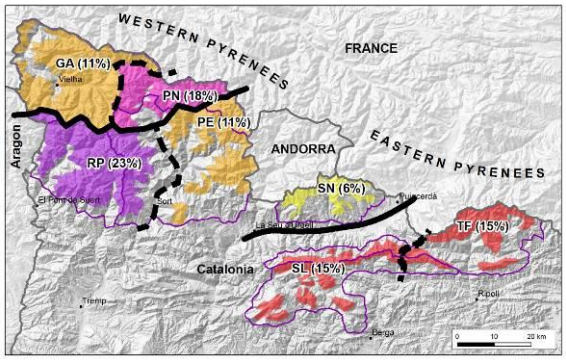

Figure 11. MAR defined from the frequency and spatial distribution of the registered MAE. Frequency of MAE occurrence in P3 is indicated in brackets. Black lines indicate main divisions and dashed black lines, secondary divisions.

4.2 Analysis of P2+P3 period

To characterize episodes recorded during P2+P3 period, we worked at winter season time resolution in order to adapt to P2 data limitations. Since the dataset was not complete, the calculation of the AMI was simplified considering the minimum frequency obtained from all the MA registered per winter in each MAR, according to the expression 2.

$$SAMI = \sum_{i=1}^{3} \frac{min(Fw_i)}{3 \cdot 3} \qquad (2)$$

This index was called Simplified Avalanche Magnitude Index (SAMI), where min(Fw) corresponds to the lowest frequency of the MA recorded in one winter (*w*) for each of the 3 CMAR (*i* stands for these regions). A low correlation AMI*w*-SAMI forced us to simplify the 7 MAR to 3 CMAR for which the Pearson correlation was 0,80. The weight for the estimated frequencies (again, 0.1, 0.3, 1 and 3 from high to very low frequency MA) was assigned in order to highlight the less probable episodes. Divisor values correspond to the maximum value of the frequency (3) and maximum number of CMAR (3) for the standardization of the data.

The SAMI is a simplification of the AMI devised in case of less complete data series. It is based on the assumption that larger destructive avalanches are easier to remember than high frequency avalanches. Hence, the result has to be interpreted as an approximation. It highlights the maximum values registered in each region and therefore those episodes with low frequency

MA and less extensive, against very extensive episodes but with high frequency MA.

In figure 12 the calculated SAMI values for P2+P3 are represented. Winter season 1995/96 shows the highest SAMI value, while the episodes of 1971/72, 1974/75, 1937/38, 2004/05, and 2005/06 have high SAMI values (in decreasing order), together with 12 other winters bordering the value 0.1. The remaining recorded MAE (25 winters) register medium and low SAMI values.

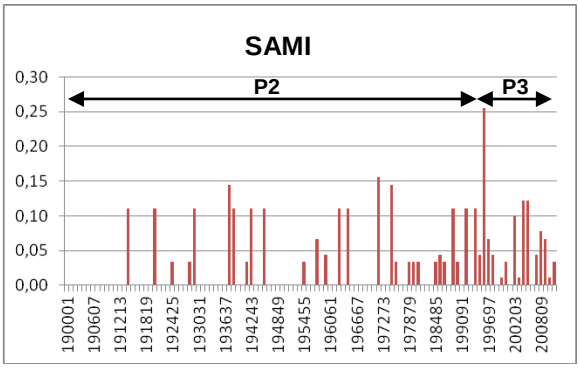

Figure 12. SAMI values obtained for P2+P3 period.

4.2.2 Spatial analysis

Given the lack of information in P2, it was not possible to reach the same level of accuracy for the data set P2+P3. In many cases, the period P2 only registers one MA per winter. In this case the value 1 was assigned to the MAR that at least recorded a MA per winter. The results (Figure 13) show how for P2+P3, GA is the region where MAE were registered more often, followed by RP, PN and TF. Regions PE and SL were affected in a similar way and finally SN was the less affected region.

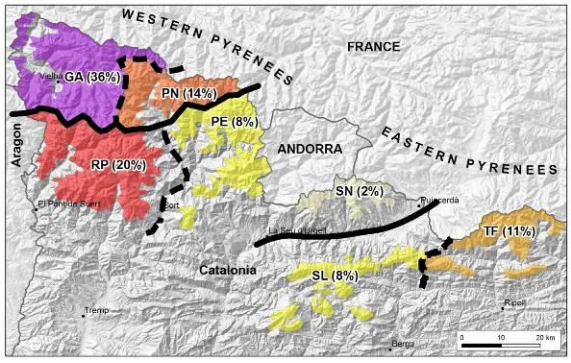

Figure 13. Frequency of MAE obtained for the period P2+P3 (values in brackets).

5 DISCUSSION

The Avalanche Magnitude Index (AMI) has allowed for the first time, to quantify the magnitude of avalanche episodes over the Pyrenees of Catalonia. We consider it a significant result because it allows quantifying and comparing the magnitude of avalanche episodes over a desired or possible time period. The results show that the episodes of January and February 1996 are still the greatest known in the last 17 years, and possibly two of the greatest in the last 100 years, as already indicated by Muntán et al. (2009), for the last 40 years.

The SAMI index is a simplified resource when not much data is available and allows to quantify the magnitude of MAE at winter season resolution. It is based on the identification of the lower frequency MA recorded for each MAR per winter. It allowed us to reconstruct the series of the twentieth and early twenty-first centuries, although it is not complete.

The analysis of the frequency, distribution and extent to which MAEs affect the study area has enabled us to define 7 MAR different to the current NR, more adjusted to MAE extent and frequency. These regions improve the characterization of the MAE, but do not replace the existing NR, which are also used for high and very high-frequency events (not dealt with in this work), and which were defined for the communication of regional avalanche forecasting.

Regarding the frequency with which the different atmospheric circulation patterns defined by García et al. (2009) took place in P3, the component 5 (S/SW, table 1) has been more times observed than in the work of the named authors, although component 1 (N/NW) is the most registered, as is also indicated by these authors. The time window is different and the selection criteria of MAE too, and these facts could have an influence on these results. Further analysis should clarify the reason for these differences.

The results in P2+P3 are similar to the results obtained in P3 period (Figures 11 and 13) for all MAR except for GA and RP regions. A surprising result, was the high MAE frequency registered in RP region in P3 (23%), since it contradicts the results obtained so far for longer periods (Garcia et al., 2007, this work for P2+P3 period). Furthermore, P2+P3 shows a positive deviation towards the GA region, not observed at P3. Garcia et al (2007) obtained similar results for the period 1939-2006. In our opinion this contradiction could be due to three factors: (i) the deviation caused by data obtained through inquiries in P2, which favours the collection of data from historically higher populated areas, (ii) the incompleteness of the P2 series, and (iii) the climate variability typical of this area, which makes atmospheric circulation to have different patterns at multiannual resolution, in relation to the relatively short time period analyzed in P3. We

believe that a longer dataset would allow checking these results.

6 CONCLUSIONS

The AMI allows determining the magnitude of MAE based on available data. It facilitates comparing episodes, obtaining frequencies, and if the series are long enough, should allow finding trends.

This index is useful for risk analysis in major avalanche events, both in forecasting and in crisis management. It can be used to define risk scenarios for civil protection.

The new regions described in this work, MAR, allow a better characterization of MAE activity over the Catalan Pyrenees.

Region RP is where more MAE and with the greatest AMI*e* values were registered. The frequency of affectation is higher than in the GA region, which registers even less frequency than regions PN, SL and TF. The GA region, despite being the area with highest snow precipitation of the Catalan Pyrenees, does not register so many frequent episodes as PR, PN, SL and TF. In the future, a larger dataset should be used to check these results.

In P2 there was a significant number of MA that could not be dated at enough time resolution to be dealt with in this paper. In the future intensive efforts will be required to rebuild this part of the series and improve our knowledge. We still can get more information on the field survey, and especially by using dendrochronology. In the same way, the study of P1 should help us to better understand the situations that generate the lowest frequency avalanches, recorded in this period, and establish whether they can happen again.

Acknowledgements: The authors are grateful to the following institutions: Conselh Generau d'Aran, FGC-Vall de Núria, Cos d'Agents Rurals, Consell Cultural de les Valls d'Àneu, Aran Culturau SCP, Registro Estatal de Accidentes por Alud, Associació per al Coneixement de la Neu i les Allaus, Arxiu Izard-Llonch i Forrellad.

7 REFERENCES

Carreras, J., Carrillo, E., Masalles, R., Ninot, J., Soriano, I., Vigo, J., 1996. Delimitation of the supra-forest zones in the Catalan Pyrenees. Bull. Soc. Linn. Provence 47, 27–36

Corona, C., Lopez, J., Stoffel, M., Bonnefoy, M., Richard, D., Astrade, L., Berger, F. (2012). How much of the real avalanche activity can be captured with tree rings? An evaluation of classic dendrogeomorphic approaches and comparison with historical archives. Cold Regions Science and Technology 74-75. 31-42.

García, C., Martí, G., Oller, P., Moner, I., Gavaldà., J., Martínez, P., Peña, J. C. (2009). Major avalanches occurrence at regional scale and related atmospheric circulation patterns in the Eastern Pyrenees. Cold Regions Science and Technology 59 (2009) 106-118.

Haegeli, P., and McClung, D.M. (2003). Avalanche characteristics of a transitional snow climate - Columbia Mountains, British Columbia, Canada. Cold Regions Science and Technology, 37, 255-276.

Mears, A.I. (1992) Snow-avalanche hazard analysis for land use planning and engineering. Colorado Geological Survey, Denver. 55 pp.

McClung, D.M. (2008). Risk-based Land-Use planning in snow avalanche terrain. In: J. Locat, D. Perret, D. Turmel, D. Demers et S. Leroueil, (2008). Comptes rendus de la 4e Conférence canadienne sur les géorisques: des causes à la gestion. Proceedings of the 4th Canadian Conference on Geohazards : From Causes to Management. Presse de l'Université Laval, Québec, 594 p.

McClung, D.M., Schaerer, P. (2006). The Avalanche Handbook (3rd edition). The Mountaineers Books. Seattle. 342 pp.

Muntán, E., Andreu, L., Oller, P., Gutiérrez, E., and Martínez, P. (2004). Dendrochronological study of the avalanche path Canal del Roc Roig, First results of the ALUDEX project in the Pyrenees, Ann. Glaciol., 38, 173–179.

Muntán, E., Garcia, C., Oller, P., Marti, G., Garcia, A., Gutierrez, E., 2009. Reconstructing snow avalanches in the Southeastern Pyrenees. Natural Hazards and Earth System Science 9, 1599–1612.

Oller, P.; Marturià, J.; González, J.C.; Escriu, J.; Martínez, P (2005): El servidor de datos de aludes de Cataluña, una herramienta de ayuda a la planificación territorial. In proceedings of: VI Simposio Nacional sobre Taludes y Laderas Inestables. Valencia, 21-24 de Junio de 2005. E. P. 905-916.

Oller, P., Muntán, E., Marturià, J., García, C., García, A., Martínez, P. (2006). The avalanche data in the Catalan Pyrenees. 20 years of avalanche mapping. Proceedings of the 2006 International Snow Science Workshop, Telluride, Colorado. Pp 305-313.

Schaerer, P. (1986):Winter weather. Weather patterns for major avalanches. The Avalanche Review, Vol. 4, No. 3.

Schweizer, J., Jamienson, B., Skjonsberg, D. (1998). Avalanche forecasting for transportation corridor and backcountry in Glacier National Park (BC, Canada). Proceedings of the 25 years of snow avalanche research (Voss, Norway, 12-16 May 1998). E, Hestnes Ed. Norwegian Geotechnical Institute. 238-243.

Weir, P. (2002). Snow avalanche management in forested terrain. Res. Br., B.B. Min. For., Victoria, B.V. Land Manage. Handb. No. 55.